Excited state hydrogen transfer dynamics in substituted phenols and their complexes with ammonia: $\pi\pi^*$-$\pi\sigma^*$ energy gap propensity and *ortho*-substitution effect

G. A. Pino,[1] A. N. Oldani,[1] E. Marceca,[2] M. Fujii,[3] S.-I. Ishiuchi,[3] M. Miyazaki,[3] M. Broquier,[4] C. Dedonder,[4,a)] and C. Jouvet[4]
[1]*INFIQC-Dpto. de Fisicoquímica, Fac. de Cs. Químicas, Universidad Nacional de Córdoba, Ciudad Universitaria, Córdoba 5000, Argentina*
[2]*INQUIMAE-DQIAQF, Fac. de Ciencias Exactas y Naturales, Universidad de Buenos Aires, Ciudad Universitaria, Pabellón II, Buenos Aires C1428EHA, Argentina*
[3]*Chemical Resources Laboratory and Integrated Research Institute, Tokyo Institute of Technology, 4259 Nagatsuta, Midori-ku, Yokohama 226-8503, Japan*
[4]*Centre Laser de l'Université Paris Sud (CLUPS) and ISMO-CNRS, Univ. Paris Sud 11, Orsay Cedex F-91405, France*

(Received 15 June 2010; accepted 28 July 2010; published online 27 September 2010)

Lifetimes of the first electronic excited state (S_1) of fluorine and methyl (*o*-, *m*-, and *p*-) substituted phenols and their complexes with one ammonia molecule have been measured for the 0^0 transition and for the intermolecular stretching σ^1 levels in complexes using picosecond pump-probe spectroscopy. Excitation energies to the S_1 ($\pi\pi^*$) and S_2 ($\pi\sigma^*$) states are obtained by quantum chemical calculations at the MP2 and CC2 level using the aug-cc-pVDZ basis set for the ground-state and the S_1 optimized geometries. The observed lifetimes and the energy gaps between the $\pi\pi^*$ and $\pi\sigma^*$ states show a good correlation, the lifetime being shorter for a smaller energy gap. This propensity suggests that the major dynamics in the excited state concerns an excited state hydrogen detachment or transfer (ESHD/T) promoted directly by a S_1/S_2 conical intersection, rather than via internal conversion to the ground-state. A specific shortening of lifetime is found in the *o*-fluorophenol-ammonia complex and explained in terms of the vibronic coupling between the $\pi\pi^*$ and $\pi\sigma^*$ states occurring through the out-of-plane distortion of the C–F bond. © *2010 American Institute of Physics*. [doi:10.1063/1.3480396]

I. INTRODUCTION

Excited state hydrogen detachment (ESHD) is a key mechanism in the photochemistry of aromatic molecules containing substituents with heteroatom(s) and excited state hydrogen transfer (ESHT) is the equivalent mechanism in clusters formed of these aromatic molecules with H acceptor solvent molecules.[1,2] The ESHT mechanism was evidenced from the generation of long-lived species occurring after the photoexcitation of phenol$(NH_3)_n$ clusters, the long-lived species being neutral $NH_4(NH_3)_{n-1}$ radicals, indicating that a photoinduced hydrogen transfer reaction takes place from the aromatic acid to the solvent moiety.[3–5] This reaction was proved to take place in clusters of $(NH_3)_n$ with several aromatic photoacid molecules.[6–11] Later, ESHD was evidenced from the release of fast H atoms after photoexcitation of bare photoacid molecules, including phenol (PhOH),[2,12,13] and substituted PhOHs,[14–16] pyrrole,[17,18] indole[19–21] and substituted indoles,[20] etc.

It has been accepted that the X-H (X=O,N,S) bond fission occurs on a potential energy surface of $\pi\sigma^*$ character, which is dissociative along the X-H coordinate.[1,2] However, in most of the molecules, the $S_2(\pi\sigma^*)$ state locates significantly higher in energy than the $S_1(\pi\pi^*)$ state, which provides most of the transition strength. The $\pi\pi^*$ state is bound along the X-H coordinate, which results in a $\pi\pi^*/\pi\sigma^*$ conical intersection (CI) at an intermediate X-H distance. The $\pi\sigma^*$ state also develops a second conical intersection with the ground $S_0(\pi\pi)$ state at longer X-H bond distances.

In 2002, the SDDJ model (model A) (Ref. 1) was introduced, which was able to explain, among many other observations, the variation of the S_1 lifetime of PhOH upon deuteration and complexation with H_2O and NH_3, in terms of the $\pi\pi^*$-$\pi\sigma^*$ and $\pi\sigma^*$-$\pi\pi$ conical intersections. Photoexcitation to the $\pi\pi^*$ state, below the energy barrier generated by the first CI, is followed by a hydrogen tunneling mechanism from the $\pi\pi^*$ to the $\pi\sigma^*$ state, in which the σ^* orbital, localized on the –OH (or –NH) group, promotes the neutral radical dissociation of the OH (or NH) bond in competition with internal conversion (IC) to the ground-state via the second CI. The competition between OH (or NH) bond dissociation and IC via the $\pi\pi$-$\pi\sigma^*$ CI is essential for the photostability of biomolecules.[1]

Despite the large energy gap between the locally excited $\pi\pi^*$ state and the $\pi\sigma^*$ in the bare photoacid molecules, the H atoms produced as a result of OH (or NH) bond cleavage are observed when the molecules are excited near their 0_0^0 transition.[2,12–21] In the case of PhOH, fast H atoms with well-defined kinetic energy have been measured[2,12] whereas in the deuterated species slow D atoms have been detected[12] indi-

a)Author to whom correspondence should be addressed. Electronic mail: claude.dedonder-lardeux@u-psud.fr.

cating that D loss occurs mostly through IC, via a statistical fragmentation which is compatible with a less efficient tunneling process for D atoms.

Later in 2006, model A was dismissed, at low excitation energies, by Ashfold and co-workers[2,12] on the basis that the $\pi\pi^*$-$\pi\sigma^*$ energy barrier is too high to be tunneled efficiently by the H atoms. Thus, a two steps model (model B)[2,12] was proposed by these authors to explain the kinetic energy of the H atom released after excitation of PhOH and substituted PhOHs excited below the top of the energy barrier. In model B, fragmentation is argued to involve successive radiationless transitions: $S_1(\pi\pi^*) \rightarrow S_0(\pi\pi)$ IC and subsequent transfer to the $S_2(\pi\sigma^*)$ potential energy surface (PES) by nonadiabatic coupling near the $\pi\pi^*$-$\pi\sigma^*$ CI. It was suggested that high ν_{OH} levels of the $S_0(\pi\pi)$ state act as efficient acceptor modes in the IC process.[12,22] The O–D stretch vibration has a lower frequency, so the corresponding conversion from $S_1(\pi\pi^*)$ to high ν_{OD} $S_0(\pi\pi)$ vibrational levels in PhOD will involve higher quantum numbers with less constructive overlap: deuteration will reduce the IC probability to $S_0(\pi\pi)$.[12,22] Thus, in model B, the $S_1(\pi\pi^*)$ lifetime is independent of the properties of the $S_2(\pi\sigma^*)$ state.

In clusters with polar molecules,[3–11] the ESHT mechanism has been interpreted in the framework of model A. In these cases, the polar $\pi\sigma^*$ state is significantly more stabilized than the $\pi\pi^*$ state and consequently these states cross at lower energies. Thus, in solvated clusters, ESHT followed by radical detachment takes place at lower energies. This interpretation is consistent with a number of data;[1,3–10,23–25] however a systematic examination of the ESHD/T model should still be performed to discriminate the validity of models A and B.

According to model A, the excited state lifetime of the photoacid molecules and their complexes will necessarily depend on the energy gap between the $\pi\pi^*$ and $\pi\sigma^*$ states; on the other hand, the influence of the $\pi\sigma^*$ state properties on the S_1 lifetime is less evident in model B, particularly in the Franck–Condon region which is probed here. Therefore, it should be interesting to determine the excited state lifetimes of a group of molecules and complexes with varying $\pi\pi^*$-$\pi\sigma^*$ energy gaps, in order to find out whether or not there is a correlation between these properties. Substitution on the aromatic ring of PhOH modifies the energy of the ground and excited electronic states and is then a way to modify the potential barrier energy at the $\pi\pi^*$-$\pi\sigma^*$ CI.

In a previous work,[8] we focused on the effect of fluorine on the ESHT reaction in *o*-, *m*-, and *p*-fluorophenol$(NH_3)_n$ (F-PhOH$(NH_3)_n$) clusters as the first step of a systematic study. The resonance effect of fluorine causes a mild perturbation to the π electron system of the aromatic ring and consequently substitution of an H atom by fluorine does not introduce major changes in the vibrational modes pattern. The observed perturbation in the vibrational modes involving the OH group is partly due to the proximity of the fluorine atom in the ring, which withdraws electron density by inductive effect through the σ_{C-F} bond. From the comparison between the $(1+1')$ REMPI spectra and the action spectra obtained by monitoring the reaction products $NH_4(NH_3)_{n-1}$, we were able to suggest that, for excited F-PhOH$(NH_3)_n$ clusters, the ESHT reaction becomes faster in the order *m*-, *p*-, and *o*-.[8]

In the case of methylphenols (cresols, CH_3-PhOH), phenolic skeletal vibrational modes do not differ much from those found in F-PhOHs as a result of the similar mass of CH_3 and F groups. The methyl group is an electron-donor group that introduces electronic charge in the π orbitals by hyperconjugation.[26] The effect of the CH_3 group on the excited state lifetime of *p*-CH_3-PhOH(NH_3) (Ref. 10) and *p*-CH_3-PhOH$(H_2O)(NH_3)$ (Ref. 9) complexes was studied by comparing the relative intensities of the different transitions in the REMPI (1+1) and LIF spectra. While vibrational-mode specificity was reported for PhOH(NH_3), the lifetime of the S_1 state of the *p*-CH_3-PhOH(NH_3) complex decreases monotonically upon vibrational excitation. This result was interpreted as a more statistical behavior of the latter complex, as a consequence of a stronger coupling of the intermolecular σ mode with the low frequency vibrational modes introduced by the CH_3 group.[10]

Ashfold and co-workers[15] studied the photodissociation of bare *o*-, *m*-, and *p*-CH_3-PhOH by H (Rydberg) atom photofragment translational (HPT) spectroscopy. Due to the increased density of states resulting from the introduction of a CH_3 group in the PhOH moiety, these authors expected an enhancement in the intramolecular vibrational redistribution (IVR) rate following internal conversion to the ground-state, as compared to PhOH. However, in the HPT spectra a structured feature at high kinetic energies was found, revealing vibrational specificity in the methylphenoxy radicals, for all the compounds,[15] as in the case of PhOH.[12] These results indicate that the OH bond dissociation takes place faster than IVR. In the framework of model B, it was interpreted that $S_1(\pi\pi^*) \rightarrow S_0(\pi\pi)$ IC is slow, but when the S_0 potential energy surface is accessed, the subsequent dissociation with sufficient energy in the appropriate motions to sample the $\pi\pi/\pi\sigma^*$ CI is fast compared to the competing IVR process.[15] Similar experimental results were observed by Tseng *et al.*[16] in the photodissociation of *p*-CH_3-PhOH by multimass ion imaging technique, but the process was explained in terms of model A. Studies on the ESHD by H (Rydberg) atom photofragment translational spectroscopy in bare *p*-F-PhOH and other *para* halogenated PhOHs,[14] have shown similar results to those obtained on bare PhOH (Ref. 12) and *o*-, *m*-, and *p*-CH_3-PhOH.[15]

The dependence of the S_1 state lifetime on the position of the F atom in *o*-, *m*-, and *p*-F-PhOH(NH_3) (Ref. 8) and the effect of the CH_3 group in *p*-CH_3-PhOH(NH_3) (Ref. 10) have been qualitatively explored using nanosecond lasers. Measurements of excited state lifetimes and reaction rates would be necessary to complete the description of these systems. In the present work, we have performed pump-probe picosecond experiments to measure the excited state lifetimes of fluorine and methyl substituted phenols in *o*-, *m*-, and *p*-positions, as well as the lifetimes of their complexes with one ammonia molecule, in order to clarify the position effect and the substituent effect. Since these two substituents have different electronic characters, they are expected to produce different energy shifts in the $\pi\pi^*$ and $\pi\sigma^*$ states. This

should be clearly evidenced in the measurement of the ESHD/T reaction rate provided that the reaction mechanism is linked to the relative energy of these two electronic states. The ESHD/T mechanism will be discussed on the basis of the measured lifetimes and their correlation with the energy gaps calculated between the $\pi\pi^*$ and $\pi\sigma^*$ states.

II. EXPERIMENTAL

Jet-cooled molecules and their clusters were generated by expanding neat He or a mixture of He seeded with NH_3 ($<1\%$), in which the substituted phenol was added by passing the gaseous mixture over a reservoir containing the molecule under study at room temperature. The backing pressure was typically 1 bar and the gaseous mixture was expanded to vacuum through a 300 μm diameter pulsed nozzle (solenoid general valve, series 9). Under these conditions, no large clusters were observed and structured vibronic REMPI $(1+1')$ spectra were obtained. Fluoro and methyl (*o*-, *m*-, and *p*-) substituted phenols from Sigma-Aldrich Chemie S.a.r.l. (L'Isle d'Abeau Chesnes, 38297 Saint-Quentin Fallavier, France) were used without further purification.

The unskimmed free jet was crossed at right angle by the copropagated excitation and ionization laser beams, 10 cm downstream from the nozzle. The interaction region was the center of the extraction zone of a linear time-of-flight mass spectrometer. The produced ions were accelerated perpendicularly to the jet axis toward a microchannel plates detector located at the end of a 1.5 m field-free flight tube.

The third harmonic (355 nm) output of a mode-locked picosecond Nd:YAG laser [EKSPLA-SL300 (LT-02300 Vilnius, Lithuania)] was split into two parts in order to pump two optical parametric amplifiers (OPA) with second harmonic generation (SHG) systems (EKSPLA-PG411) to obtain tunable UV light. One of the systems was used as the excitation laser (ν_1) tuned on the different transitions of the molecules and clusters studied. The energy of the ν_1 laser was attenuated to preclude one-color two-photon ionization. The other OPA-SHG system was tuned to 295 nm and used as the ionization laser (ν_2), keeping the energy to approximately 120 μJ/pulse. The temporal shapes of both pulses were determined in the fitting procedure to be Gaussian curves having full width at half height (FWHH) of 10 ps, while the spectral linewidth was 5 cm^{-1}. Both laser pulses were optically delayed between -350 and 1350 ps by a motorized stage.

Since the lifetime of the molecules and some of the complexes studied in this work are in the order of a few nanoseconds, special care was taken to ensure a correct alignment of both laser beams and avoid the appearance of artifacts in the pump-probe delay curve. The excited state lifetime for the origin transition of toluene is known to be 86 ns,[27] meaning that this transition should provide a step function within the first 1.35 ns that can be recorded in the experiment. The measurement of this step function for the excited state lifetime of toluene was used as a criterion for a good alignment of the laser beams and gives the cross correlation of the laser temporal widths.

III. THEORETICAL CALCULATION

The calculations were performed with the TURBOMOLE program package,[28] making use of the resolution-of-the-identity (RI) approximation for the evaluation of the electron-repulsion integrals[29] in the MP2 and CC2 calculations.

The ground-state equilibrium geometries of F-PhOHs and CH_3-PhOHs molecules and their complexes with ammonia were determined using the MP2 method. Vertical excitation energies, oscillator strengths, and dipole moments were calculated at the ground-state equilibrium geometry with the CC2 method,[30] using Dunning´s correlation-consistent split-valence double-zeta basis set with polarization functions on all atoms (aug-cc-pVDZ).[31]

In these calculations, the starting geometries were constructed with Cs symmetry constraint to distinguish between π and σ orbitals and A′ and A″ excited states. In addition to the ground-state geometry optimizations and vertical excitation energy calculations, the geometries of the lowest excited states, which in all the cases studied here correspond to $A'(\pi\pi^*)$ states, were optimized in Cs symmetry. The energies of the ground and the first $A''(\pi\sigma^*)$ states were also calculated for the optimized $A'(\pi\pi^*)$ excited state geometries. The excited state optimizations were performed at the RI-CC2 level with the aug-cc pVDZ basis set that is required to describe the Rydberg nature of the σ^* orbitals. In the case of *ortho* complexes with ammonia, additional excited state optimizations were performed starting from non-planar geometries.

IV. RESULTS

A. Pump-probe experiments and excited state lifetimes

The excited state lifetimes of *o*-, *m*-, and *p*-F-PhOH and *o*-, *m*-, and *p*-CH_3-PhOH and their clusters with one NH_3 molecule were measured upon excitation to the S_1 origin as well as to the σ^1 vibronic level corresponding to the intermolecular stretching mode in the ammonia complexes. The S_1 lifetimes of *m*-F-PhOH, *m*-F-PhOH(NH_3), *m*-CH_3-PhOH, and *m*-CH_3-PhOH(NH_3) were measured for the *cis* (c) and *trans* (t) isomers. For *o*-F-PhOH, we only had access to the *cis* isomers of the bare molecule and of the 1:1 ammonia complex since, in agreement with the observation of other authors,[32,33] the *trans* isomers are not present in the expansion. For *o*-CH_3-PhOH, we were able to measure the S_1 lifetime of the *cis* and *trans* isomers, while only the t,*o*-CH_3-PhOH(NH_3) complex was observed.

Figures 1 and 2 show the $(1+1')$ time evolution of the intensity corresponding to the mass-resolved and spectroscopically selected ionization signal for the different molecules and complexes studied. The data were fit by convoluting a single exponential decay function with the laser pulses shapes. The best fits are also shown in the same figures together with the residual errors.

Although the expansion conditions were adjusted to avoid the formation of large clusters, it must be noticed that the vibrational bands resulting from *o*-F-PhOH(NH_3), *o*-CH_3-PhOH(NH_3), and *m*-CH_3-PhOH(NH_3) complexes are

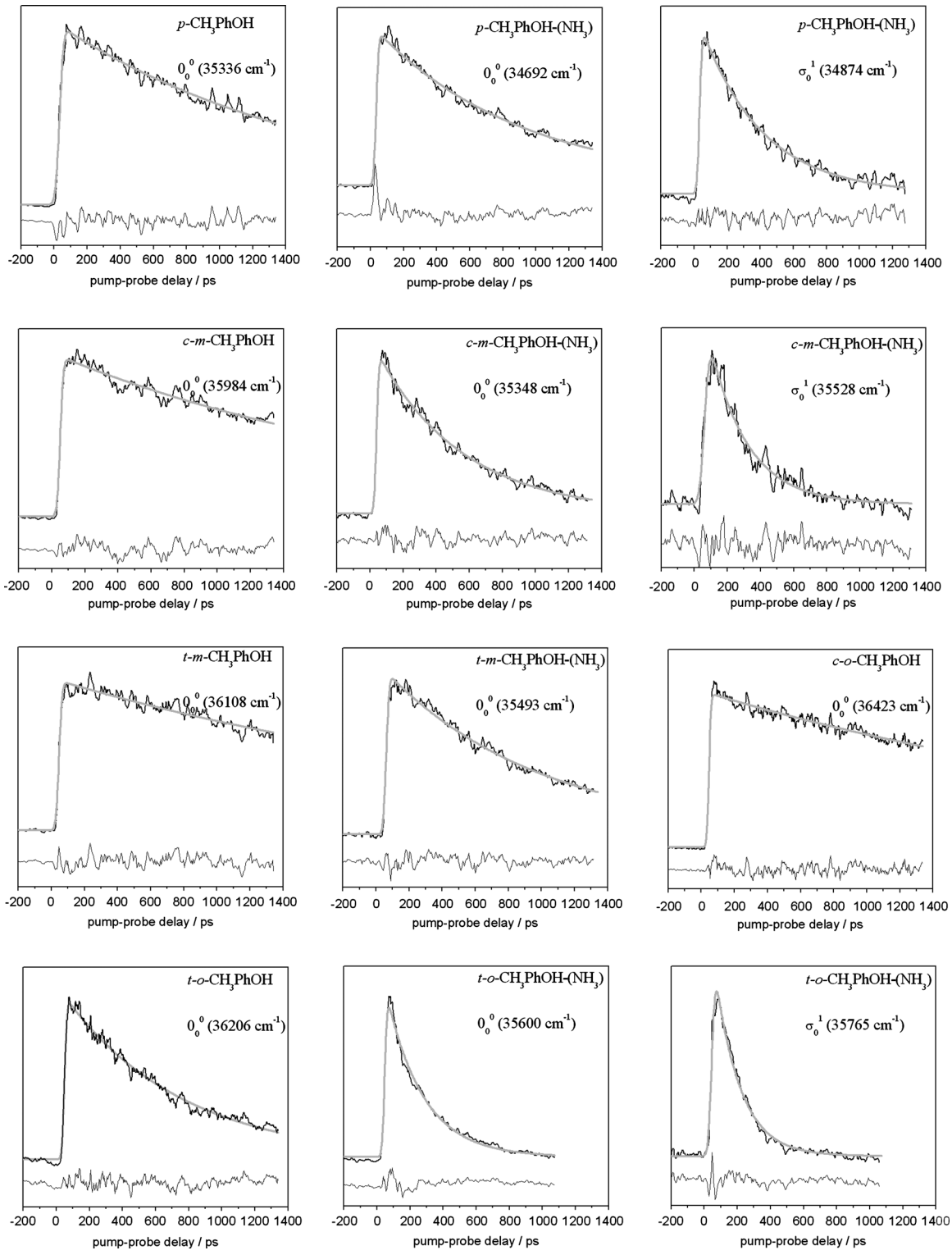

FIG. 1. Excited state time evolution (—) for the CH_3-PhOH isomers and their complexes with one ammonia molecule, as labeled in each panel together with the best fit (grey line). The lower trace of each panel shows the residual error (—) between the experimental and the fitting results. The pump laser was tuned on the 0_0^0 transition of the free molecules and on the 0_0^0 and σ_0^1 transition of the complexes with the probe laser set at 295 nm. All the traces have been corrected by subtracting the background signal as mentioned in the text.

superimposed on a background due to the excitation of larger clusters, probably 1:2 complexes. To extract the actual signal of the 1:1 complexes, decay curves recorded by exciting at the bottom of each band were subtracted from the total signal recorded when the pump laser was tuned at the center of each vibrational transition. This procedure has been applied in previous papers and was found to be adequate for this purpose.[3,25]

The measured S_1 lifetimes are depicted in Table I. For comparison, values reported by other authors[25,34–37] are also

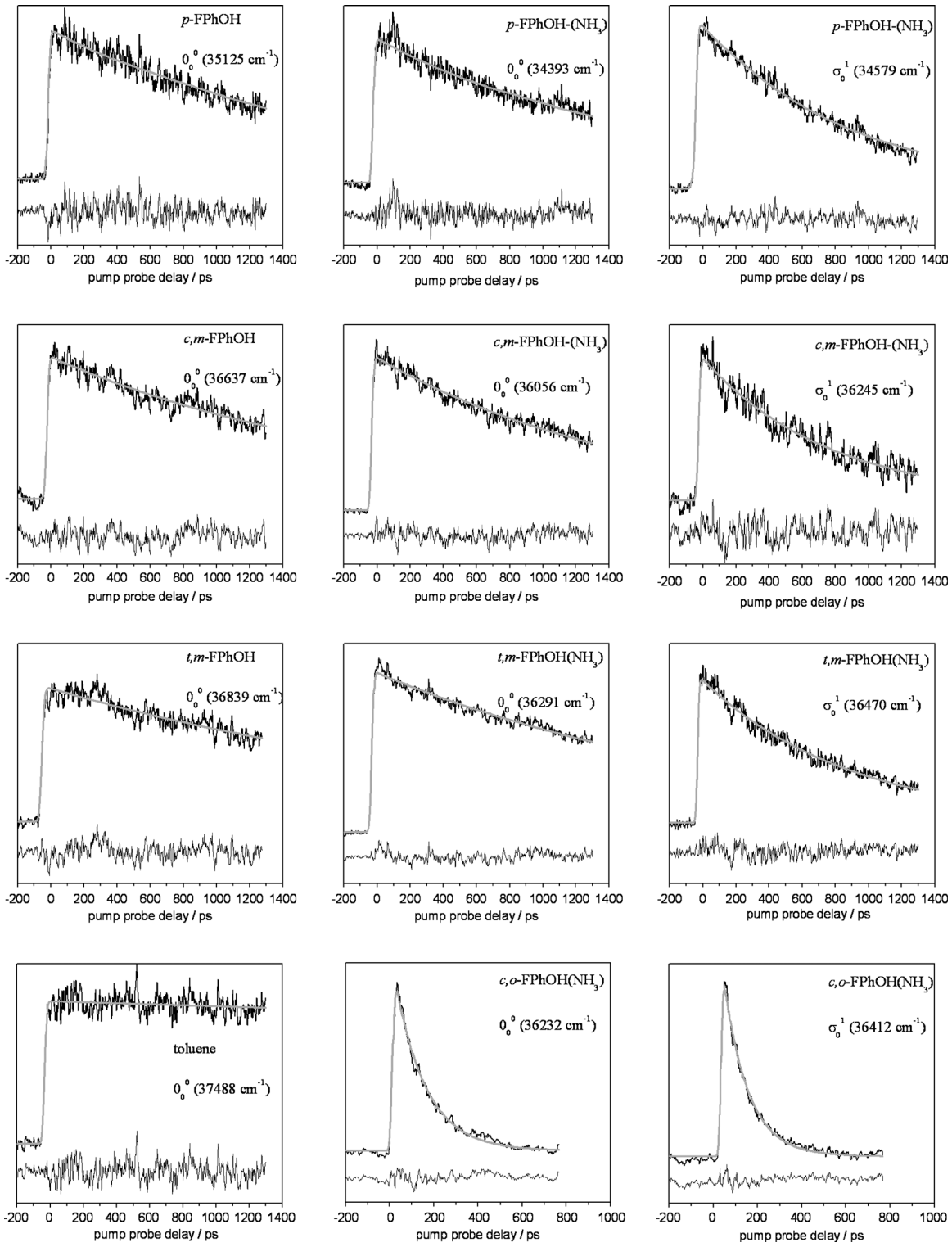

FIG. 2. Excited state time evolution (—) for the F-PhOH isomers and their complexes with one ammonia molecule and bare toluene, as labeled in each panel together with the best fit (grey line). The lower trace of each panel shows the residual error (—) between the experimental and the fitting results. The pump laser was tuned on the transition 0_0^0 transition of the free molecules and on the 0_0^0 and σ_0^1 transition of the complexes with the probe laser set at 295 nm. All the traces have been corrected by subtracting the background signal as mentioned in the text.

shown in the same table, as well as the values corresponding to PhOH and PhOH(NH_3) that were also redetermined in this work.

Several features should be noticed from the inspection of Table I:

(1) The effect of complexation is more important in CH_3-PhOHs than in F-PhOHs.

(2) The lifetimes of the 1:1 ammonia complex involving *ortho*-substituted PhOHs are always the shortest in each series.

(3) The excited state of the c,*o*-F-PhOH(NH_3) complex is extremely short lived (140 ps) as compared with the S_1 lifetime of the other members of the F-PhOH series (nanosecond scale).

TABLE I. Excited state lifetimes of the *o*-, *m*-, and *p*- (CH_3 and F) substituted phenols and their complexes with one ammonia molecule, together with the excited state lifetimes of the deuterated species collected in the literature.

	X-PhOH bare molecule 0_0^0 excitation τ (ns)	X-PhOH(NH_3) complex 0_0^0 excitation τ (ns)	X-PhOH(NH_3) complex σ_0^1 excitation τ (ns)	X-PhOD bare molecule 0_0^0 excitation τ (ns)
p-CH_3-PhOH	1.7 ± 0.1, 1.6 ± 0.2 [a]	0.89 ± 0.03	0.37 ± 0.03	9.7[a]
c,*m*-CH_3-PhOH	2.4 ± 0.1	0.50 ± 0.03	0.23 ± 0.02	9.8[b]
t,*m*-CH_3-PhOH	3.0 ± 0.2	0.91 ± 0.05		26.7[b]
c,*o*-CH_3-PhOH	3.0 ± 0.2			14.9[b]
t,*o*-CH_3-PhOH	0.70 ± 0.03	0.22 ± 0.02	0.14 ± 0.02	10.6[b]
PhOH	2.2 ± 0.1, 2.4 ± 0.3 [c]	1.1 ± 0.1, 1.2 ± 0.2 [d]	0.45 ± 0.08, 0.39 ± 0.09 [d]	13.3[c]
p-F-PhOH	1.7 ± 0.1, 1.8 ± 0.1 [e]	1.7 ± 0.2	0.87 ± 0.06	3.2[e]
c,*m*-F-PhOH	1.9 ± 0.1	1.6 ± 0.2	0.75 ± 0.05	(*3.3*[g])
t,*m*-F-PhOH	2.7 ± 0.2	2.4 ± 0.1	0.84 ± 0.05	(*8.9*[g])
c,*o*-F-PhOH	4.6 ± 0.1 [f]	0.14 ± 0.01	0.11 ± 0.02	(*5.0*[g])

[a]Reference 34.
[b]Reference 35.
[c]Reference 37.
[d]Reference 25.
[e]Reference 36.
[f]Reference 33.
[g]These values are not available in bibliography. Thus, it was assumed that the ratios $\tau_{o\text{-F-PhOD}}/\tau_{p\text{-F-PhOD}}$ and $\tau_{m\text{-F-PhOD}}/\tau_{p\text{-F-PhOD}}$ are the same than the corresponding ratios for *o*-, *m*-, and *p*-CH_3-PhOD.

As a general rule, the S_1 lifetime measured upon excitation to the σ^1 vibronic level is around twice shorter than that determined for the $S_1 \leftarrow S_0$ electronic transition origin.

B. Theoretical calculation of excitation energies and geometries

Figure 3 displays schematically the definition of the calculated quantities. Tables II and III summarize in the upper part the values of the vertical transition energies ($E_{\text{vertical}} = E0(S_1) - E0(S_0)$) and the $\pi\pi^*$-$\pi\sigma^*$ energy gaps ($\delta^{S_0}_{\pi\pi^*\text{-}\pi\sigma^*}$) calculated at the $S_0(\pi\pi)$ state optimized geometry for all the studied CH_3-PhOHs and F-PhOHs, respectively. The energy values of the A′ and A″ states, $E1(S_0)$, $E1(S_1)$, and $E1(1A'')$, calculated at the $S_1(\pi\pi^*)$ optimized geometry, the transition energy ($E_{\text{adiabatic}}$), and the corresponding $\pi\pi^*$-$\pi\sigma^*$ energy gaps ($\delta^{S_1}_{\pi\pi^*\text{-}\pi\sigma^*}$) at the $S_1(\pi\pi^*)$ optimized geometry, are tabulated in the lower part of Tables II and III.

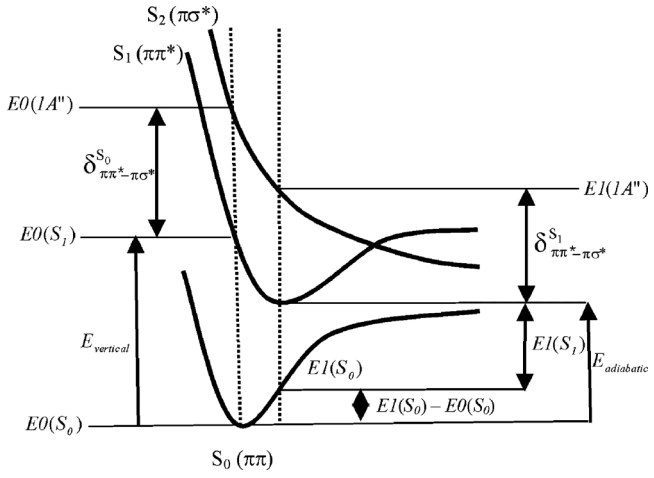

FIG. 3. Schematic representation of the relevant potential energy curves invoked in the discussion of this work and definition of the calculated quantities: vertical and adiabatic transition energies, and vertical and adiabatic energy gaps.

We note that the $\delta^{S_0}_{\pi\pi^*\text{-}\pi\sigma^*}$ and $\delta^{S_1}_{\pi\pi^*\text{-}\pi\sigma^*}$ energy gaps of PhOH are larger than those of CH_3-PhOHs and smaller than those of F-PhOHs. The adiabatic transition energies ($E_{\text{adiabatic}} = E1(S_1) - E0(S_0)$) can be compared with the experimental transition origins.

Notice that all the calculated transition energies are within 0.18 eV of the experimental values and the relative order of the $E_{\text{adiabatic}}$ is the same as the experimental values within a family of molecules. For methyl substitution, $E_{\text{adiabatic}}(p) < E_{\text{adiabatic}}(c,m) < E_{\text{adiabatic}}(t,m) < E_{\text{adiabatic}}(t,o) < E_{\text{adiabatic}}(\text{PhOH}) < E_{\text{adiabatic}}(c,o)$, where the specific isomer and substitution position are indicated in parentheses. The adiabatic transition of c,*o*-CH_3PhOH is found in the calculation 0.007 eV higher than the PhOH transition energy and this difference is in good agreement with the experimental difference of 0.011 eV. In the same way, for F-PhOHs calculations give the order $E_{\text{adiabatic}}(p) < E_{\text{adiabatic}}(\text{PhOH}) < E_{\text{adiabatic}}(c,m) < E_{\text{adiabatic}}(c,o) < E_{\text{adiabatic}}(t,m)$.

All the calculations done for the bare molecules were repeated for the 1:1 complexes of methylphenols and fluorophenols with ammonia and the results are summarized in Tables IV and V, respectively. For all these complexes, the $\pi\pi^*$-$\pi\sigma^*$ energy gaps are lower than in the bare molecules, both at the S_0 and the S_1 optimized geometries.

All the calculations have been performed by keeping the planar symmetry (Cs) except in the case of c,*o*-F-PhOH(NH_3) for which calculations in the C1 symmetry group (complete optimization) have been performed as well since, as discussed below, the molecule bends in the excited state.

V. DISCUSSION

A. Comparison between methyl and fluorine substituent

As mentioned previously, the introduction of a substituent in the aromatic ring of phenol is expected to modify strongly the energy of the ground and excited electronic states, which may perturb the potential barrier at the $\pi\pi^*$-$\pi\sigma^*$ conical intersection and, consequently, influence the photodissociation dynamics of the molecules. Comparison between Tables II and III reveals that fluorine substitution leads invariably to larger $\pi\pi^*$-$\pi\sigma^*$ energy gaps than that calculated for the phenol molecule, while methyl substitution leads to smaller energy gaps than in fluorophenols. Although the change in $\delta_{\pi\pi^*\text{-}\pi\sigma^*}$ due to the formation of 1:1 complexes with NH_3 will be discussed in the following section, we can anticipate that the substituent effect found for the bare molecules is also valid for the clusters with ammonia, the $\pi\pi^*$-$\pi\sigma^*$ energy gaps of CH_3-PhOH(NH_3) clusters being always lower than that of the PhOH(NH_3) complex, and the gaps of PhOH(NH_3) cluster being lower than those corresponding to F-PhOH(NH_3) clusters (Tables IV and V). In the following paragraphs we will discuss qualitatively the effect of fluorine and methyl substitution on the electronic orbital energies, making use of simple electrostatic arguments.

The opposite behavior of methyl and fluorine substituents on the aromatic ring relies mainly on the fact that, while methyl groups introduce electronic charge in the π orbitals by hyperconjugation,[26] fluorine causes electron withdrawal[14] from the ring (inductive effect) that is only partly compensated by the π back-donation into the aromatic system.

While the presence of an electron-donor substituent such as CH_3 causes a minor effect on the σ^* orbital centered on the O–H bond, it destabilizes the highest occupied molecular orbital (HOMO) and the lowest unoccupied molecular orbital (LUMO) of the molecular π-system to a similar extent. This is visualized in Table II, where the $A''(\pi\sigma^*)$ vertical energies for cresols are smaller than that obtained for phenol, while the $A'(\pi\pi^*)$ energies remain similar. Likewise, the $A''(\pi\sigma^*)$ energies at the S_1 geometry are found smaller for CH_3-PhOHs than for PhOH, while the calculated S_1 $A'(\pi\pi^*)$ energies are quite similar for all the molecules, with the exception of the *para* compound. Moreover, the effect of methyl substitution in 1:1 clusters with ammonia (Table IV) exhibits similar characteristics: a bathochromic shift is found for the $A''(\pi\sigma^*)$ vertical energies in the substituted complexes (at the S_0 and S_1 optimized geometries), and the energy of the S_1 $A'(\pi\pi^*)$ states (at both the S_0 and S_1 optimized geometry) shows a moderate redshift (again with a singular behavior of the *para* complex), implying that the hyperconjugative effect destabilizes more efficiently the π than the π^* molecular orbitals.

On the other hand, the fluorine substitution effect is governed by a strong electron withdrawal from the aromatic ring caused by the halogen atom; this stabilizes the HOMO orbital as well as the LUMO, but to a less extent. Consequently, at both the S_0 and S_1 optimized geometries, the $A''(\pi\sigma^*)$ and $A'(\pi\pi^*)$ energies are larger for F-PhOHs than for PhOH, the differences being smaller for the $A'(\pi\pi^*)$ state (Table III); the *p*-substituted F-PhOH is an exception, where the poorer inductive effect is compensated by the π back-donation. The same behavior is found for 1:1 F-PhOH(NH_3) clusters (Table V). Finally, we find that the overall substitution effect provokes in F-PhOHs a significant increase of the $\pi\pi^*$-$\pi\sigma^*$ energy gaps.

B. Effect of the cluster formation and σ mode excitation on the S_1 lifetime

The S_1 lifetime of all the molecules studied in this work show the same tendency upon the formation of clusters with ammonia, for which the measured values are always shorter than the monomer ones. This is consistent with model A (Ref. 1) that suggests that cluster formation preferentially stabilizes the $\pi\sigma^*$ state as compared to the $\pi\pi^*$ state, which is expected to reduce the energy barrier (width and height) making the ESHT faster. The interesting point is that this effect depends strongly on the nature of the substituent. For *m*- and *p*-F-PhOH, the effect is not significant; upon cluster formation lifetimes change from $\tau=2000$ ps to $\tau=1600$ ps for c,*m*-F-PhOH, from $\tau=2700$ ps to $\tau=2400$ ps for t,*m*-F-PhOH, and from $\tau=1700$ ps to $\tau=1600$ ps for *p*-F-PhOH. A peculiar behavior is found for c,*o*-F-PhOH where a drastic shortening of the S_1 lifetime from $\tau=4100$ ps to $\tau=140$ ps occurs; this effect is due to a specific geometrical distortion of the molecule and will be treated separately in Sec. V D. In contrast with the weak effect recorded in *m*- and *p*-F-PhOH, CH_3-PhOH shows significant lower S_1 lifetimes for all the complexes (see Table I).

As described above, larger $\pi\pi^*$-$\pi\sigma^*$ energy gaps are found in F-PhOHs than in CH_3-PhOHs due to the different effect of the F- and CH_3-groups. Moreover, in F-PhOHs $\delta_{\pi\pi^*\text{-}\pi\sigma^*}$ only decreases ~35% upon cluster formation with one ammonia molecule, while in CH_3-PhOHs $\delta_{\pi\pi^*\text{-}\pi\sigma^*}$ decreases ~65%, depending on the isomer. This implies that when F-PhOHs are solvated, the change in the barrier height and shape is less important and consequently the acceleration of the tunneling process in the ESHT reaction is small as compared to CH_3-PhOHs.

It is clear from Table I that the lifetime of the σ^1 vibronic level (i.e., the intermolecular OH···NH_3 stretching mode) is shorter than that of the origin in all the clusters. For example, in *p*-F-PhOH–(NH_3), the lifetime is shortened from 1660 to 880 ps if the σ^1 band (186 cm^{-1} from the origin) is excited. This behavior is in line with previous results on PhOH(NH_3) complexes,[25] in which excitation to the σ^1 vibronic level leads to a strong decrease of the S_1 lifetime. This effect is explained in model A (Ref. 1) by a decrease of the width of the energy barrier when the σ^1 mode is excited since this mode is linked to the reaction coordinate, leading to an increased tunneling rate.

C. Energy gap propensity on the S_1 lifetime

The S_1 lifetimes of F-PhOHs, CH_3-PhOHs, and their 1:1 complexes with ammonia are plotted versus the $\delta^{S_0}_{\pi\pi^*\text{-}\pi\sigma^*}$ and $\delta^{S_1}_{\pi\pi^*\text{-}\pi\sigma^*}$ energy gaps in Figs. 4(a) and 4(b), respectively. Both plots show that there is a good correlation between lifetime and energy gap for most of the molecules and clus-

TABLE II. Energies of the $\pi\pi^*$ (eV) and $\pi\sigma^*$ (eV) states of all the isomers of bare CH_3-PhOH at the S_0 (upper panel) and S_1 optimized geometry (lower panel) calculated at the CC2 level with the aug-cc-pVDZ basis set. All the starting geometries were constructed with Cs symmetry constraint. The values of the calculated adiabatic transition energies and the experimental transition energies (in eV) are also depicted in the table as well as the energy gap between the $\pi\pi^*$ and $\pi\sigma^*$ state at the S_0 and S_1 optimized geometries. The corresponding values for the bare phenol molecule (PhOH) are also included for comparison.

		m-CH_3-PhOH		*o*-CH_3-PhOH		
	p-CH_3-PhOH	*cis*	*trans*	*cis*	*trans*	PhOH
			S_0 optimization			
$E0(S_1)$ vertical energy ($E_{vertical}$)	4.826	4.840	4.858	4.880	4.870	4.864
$E0(1A'')$ vertical energy	5.172	5.241	5.245	5.299	5.193	5.365
$\pi\pi^*$-$\pi\sigma^*$ energy gap (vertical)	**0.346**	**0.401**	**0.386**	**0.419**	**0.323**	**0.501**
			S_1 optimization			
$E1(S_1)$ S_1 optimized energy	4.354	4.481	4.488	4.516	4.507	4.495
$E1(S_1)-E0(S_0)$ ($E_{adiabatic}$)	**4.472**	**4.638**	**4.653**	**4.680**	**4.667**	**4.673**
Experimental transition energies	***4.382***	***4.462***	***4.477***	***4.516***	***4.489***	***4.508***
$E1(1A'')$ $1A''$ energy at the S_1 geometry	5.006	5.116	5.099	5.153	5.066	5.196
$\pi\pi^*$-$\pi\sigma^*$ energy gap for optimized S_1	**0.652**	**0.635**	**0.611**	**0.637**	**0.559**	**0.523**

ters: the lifetime is longer if the calculated energy gap is larger (4500 ps/eV for a linear trend). An exception is the c,*o*-F-PhOH(NH_3) complex and this particular behavior will be discussed in Sec. V D.

The observed dependence of the S_1 lifetime on $\delta_{\pi\pi^*\text{-}\pi\sigma^*}$ can be reasonably interpreted considering that the OH bond cleavage or the ESHT reaction occur via tunneling through the barrier generated by the $\pi\pi^*$-$\pi\sigma^*$ conical intersection,[1,24,25,38] therefore the dissociation rate will be strongly dependent on the barrier height (E_h), measured from the S_1 zero-point energy, as well as on its shape, both quantities being directly related to $\delta_{\pi\pi^*\text{-}\pi\sigma^*}$.

In the framework of model A,[1] the ESHT reaction (or OH bond cleavage) is an exothermic process in which the system behaves as a "free particle" after reaching the $\pi\sigma^*$ state. Under this assumption, when the excitation energy is lower than the barrier maximum the system may: (i) proceed to the S_0 state via internal conversion and subsequent dissociation[2,12,14–17,21,39,40] or (ii) tunnel through the potential barrier.[1,5–10,24,25] We will show that the observed propensity between $\delta_{\pi\pi^*\text{-}\pi\sigma^*}$ and the measured lifetimes is compatible with the latter mechanism, while there are no apparent reasons to support the dissociation via IC.

The tunneling rate constant ($k_{tunneling}$) for a mechanism of the type (ii) can be described by the expression[41]

$$k_{tunneling} = \nu \exp\left[-\frac{a\pi}{2\hbar}(2mE_h)^{1/2}\right], \quad (1)$$

in which ν is the zero-point frequency for the hydrogen motion in the S_1 potential well, m represents the hydrogen mass, and a is the barrier half width at the S_1 zero-point energy. Since a and E_h are related to $\delta_{\pi\pi^*\text{-}\pi\sigma^*}$, $\ln(k_{tunneling})$ will follow the variation of $\delta^{S_1}_{\pi\pi^*\text{-}\pi\sigma^*}$.

TABLE III. Energies of the $\pi\pi^*$ (eV) and $\pi\sigma^*$ (eV) states of all the isomers of bare F-PhOH at the S_0 (upper panel) and S_1 optimized geometry calculated (lower panel) at the CC2 level with the aug-cc-pVDZ basis set. All the starting geometries were constructed with Cs symmetry constraint except for the case of the c-*o*-F-PhOH molecule, for which additional optimizations were performed starting from nonplanar geometries. The values of the calculated adiabatic transition energies and the experimental transition energies (in eV) are also depicted in the table as well as the energy gap between the $\pi\pi^*$ and $\pi\sigma^*$ states at the S_0 and S_1 optimized geometries. The same values for the bare phenol molecule (PhOH) are also included for comparison.

	p-F-PhOH	*m*-F-PhOH		*o*-F-PhOH			PhOH
		cis	*trans*	*cis*		*trans*	
	Cs	Cs	Cs	C1	Cs	Cs	Cs
				S_0 optimization			
$E0(S_1)$ vertical energy ($E_{vertical}$)	4.668	4.917	4.937	4.932	4.932	4.896	4.864
$E0(1A'')$ vertical energy	5.304	5.571	5.524	5.620	5.620	5.437	5.365
$\pi\pi^*$-$\pi\sigma^*$ energy gap (vertical)	**0.636**	**0.654**	**0.587**	**0.688**	**0.688**	**0.541**	**0.501**
				S_1 optimization			
$E1(S_1)$ S_1 optimized energy	4.269	4.520	4.559	3.896	4.546	4.493	4.495
$E1(S_1)-E0(S_0)$ ($E_{adiabatic}$)	**4.462**	**4.715**	**4.743**	**4.677**	**4.736**	**4.693**	**4.673**
Experimental transition energies	***4.355***	***4.543***	***4.568***	***4.565***			***4.508***
$E1(1A'')$ $1A''$ energy at the S_1 geometry	5.090	5.388	5.364	5.233/5.566[a]	5.466	5.245	5.196
$\pi\pi^*$-$\pi\sigma^*$ energy gap for optimized S_1	**0.821**	**0.868**	**0.805**	**1.337/1.670[a]**	**0.920**	**0.752**	**0.523**

[a]In this case there is no pure $\pi\pi^*$ and $\pi\sigma^*$ states since the Cs symmetry is broken and the states are mixed. The reported energy gaps correspond to the S_2-S_1 and S_3-S_1 energy gaps.

TABLE IV. Energies of the $\pi\pi^*$ (eV) and $\pi\sigma^*$ (eV) states of all the isomers of CH_3-PhOH–NH_3 complex at the S_0 (upper panel) and S_1 optimized geometry (lower panel) calculated at the CC2 level with the aug-cc-pVDZ basis set. All the starting geometries were constructed with Cs symmetry constraint. The values of the calculated vertical and adiabatic energies and the experimental transition energies (in eV) are also depicted in the table as well as the energy gap between the $\pi\pi^*$ and $\pi\sigma^*$ state at the S_0 and S_1 optimized geometries. The same values for the PhOH–NH_3 complex are included for comparison.

		m-CH_3-PhOH–NH_3		*o*-CH_3-PhOH–NH_3		
	p-CH_3-PhOH–NH_3	*cis*	*trans*	*cis*	*trans*	PhOH–NH_3
			S_0 optimization			
$E0(S_1)$ vertical energy ($E_{vertical}$)	4.617	4.692	4.703	4.803	4.773	4.767
$E0(1A'')$ vertical energy	4.857	4.971	4.991	4.992	4.886	5.059
$\pi\pi^*$-$\pi\sigma^*$ energy gap (vertical)	**0.241**	**0.279**	**0.288**	**0.189**	**0.113**	**0.292**
			S_1 optimization			
$E1(S_1)$ S_1 optimized energy	4.205	4.306	4.327	4.420	4.382	4.361
$E1(S_1)-E0(S_0)$ ($E_{adiabatic}$)	**4.403**	**4.405**	**4.505**	**4.587**	**4.484**	**4.550**
Experimental transition energies	***4.302***	***4.383***	***4.401***		***4.414***	***4.430***
$E1(1A'')$ $1A''$ energy at the S_1 geometry	4.759	4.689	4.693	4.733	4.644	4.757
$\pi\pi^*$-$\pi\sigma^*$ energy gap for optimized S_1	**0.555**	**0.383**	**0.366**	**0.312**	**0.262**	**0.396**

In order to analyze the experimental results in terms of Eq. (1), it is necessary to consider that the measured decay rate constant (k) is related with $k_{tunneling}$ according to $k=k_{radiative}+k_{IC}+k_{ISC}+k_{tunneling}$, where $k=\tau^{-1}$. Based on experiments done on deuterated PhOD,[37] CH_3-PhOD [34,35] and *p*-F-PhOD,[36] where the tunneling effect is found negligible, it can be assumed that the observed decay rate constant in –OD deuterated molecules and complexes is given by $k=k_{radiative}+k_{IC}+k_{ISC}$. Since most of the lifetimes of the deuterated species are available in the literature,[34–37] these k values can be used to extract the values of $k_{tunneling}$ from the measured lifetimes. In those cases for which the lifetime of the deuterated species are not available, it was assumed that the ratio $\tau_{o\text{-F-PhOD}}/\tau_{p\text{-F-PhOD}}$ and $\tau_{m\text{-F-PhOD}}/\tau_{p\text{-F-PhOD}}$ is the same as the corresponding ratios for *o*-, *m*-, and *p*-CH_3-PhOD. Figure 5 shows that the values of $\ln(k_{tunneling})$ derived from experimental data exhibits a *quasilinear* dependence with $\delta^{S_1}_{\pi\pi^*\text{-}\pi\sigma^*}$ and this suggests that major dynamics in the excited state is ESHT (or OH cleavage) through tunneling rather than an IC mechanism to the ground-state, with the noticeable exception of the c,*o*-F-phenol-NH_3 complex that will be treated in the next section.

D. Exceptionally short lived S_1 state in *o*-F-PhOH-(NH_3)

In the preceding sections, we highlighted that the lifetimes of c,*o*-F-PhOH(NH_3) and t,*o*-CH_3-PhOH(NH_3) are the shortest in each series, suggesting the existence of an effect associated with the presence of substituents in *ortho* position. From Figs. 4 and 5, it is observed that the very short lifetime of t,*o*-CH_3-PhOH(NH_3) is related to a small $\pi\pi^*$-$\pi\sigma^*$ energy gap and thus a very fast H tunneling. However, in the same plots, the point corresponding to the lifetime of the c,*o*-F-PhOH(NH_3) is located significantly out of the propensity line. In other words, the S_1 lifetime of this c,*o*-F-PhOH(NH_3) complex is shorter than the prediction

TABLE V. Energies of the $\pi\pi^*$ (eV) and ($\pi\sigma^*$) eV states of all the isomers of F-PhOH–NH_3 complex at the S_0 (upper panel) and S_1 optimized geometries (lower panel) calculated at the CC2 level with the aug-cc-pVDZ basis set. All the starting geometries were constructed with Cs symmetry constraint, except for the case of the c-*o* and c-*m* F-PhOH–NH_3 complexes, for which additional optimizations were performed starting from nonplanar geometries. The values of the calculated vertical and adiabatic energies and the experimental transition energies (in eV) are also depicted in the table as well as the energy gap between the $\pi\pi^*$ and $\pi\sigma^*$ state at the S_0 and S_1 optimized geometries. The same values for the PhOH–NH_3 complex are included for comparison.

	p-F-PhOH–NH_3	*m*-F-PhOH–NH_3			*o*-F-PhOH–NH_3			PhOH–NH_3
		cis		*trans*	*cis*		*trans*	
	Cs	C1	Cs	Cs	C1	Cs	Cs	Cs
				S_0 optimization				
$E0(S_1)$ vertical energy ($E_{vertical}$)	4.551	4.828	4.828	4.860	4.837	4.837	4.802	4.767
$E0(1A'')$ vertical energy	5.034	5.334	5.335	5.253	5.327	5.327	5.161	5.059
$\pi\pi^*$-$\pi\sigma^*$ energy gap (vertical)	**0.483**	**0.506**	**0.507**	**0.393**	**0.490**	**0.490**	**0.359**	**0.292**
				S_1 optimization				
$E1(S_1)$ S_1 optimized energy	4.123	4.395	4.395	4.453	3.186	4.434	4.354	4.361
$E1(S_1)-E0(S_0)$ ($E_{adiabatic}$)	**4.326**	**4.607**	**4.606**	**4.643**	**4.467**	**4.630**	**4.572**	**4.550**
Experimental transition energies	***4.265***	***4.471***		***4.500***	***4.493***			***4.430***
$E1(1A'')$ $1A''$ energy at the S_1 geometry	4.676	5.021	5.021	4.988	4.635/4.990[a]	5.057	4.826	4.757
$\pi\pi^*$-$\pi\sigma^*$ energy gap for optimized S_1	**0.553**	**0.626**	**0.626**	**0.534**	**1.449/1.800[a]**	**0.623**	**0.472**	**0.396**

[a]In this case there is no pure $\pi\pi^*$ and $\pi\sigma^*$ states since the Cs symmetry is broken and the states are mixed states. The reported energy gaps correspond to the S_2-S_1 and S_3-S_1 energy gaps.

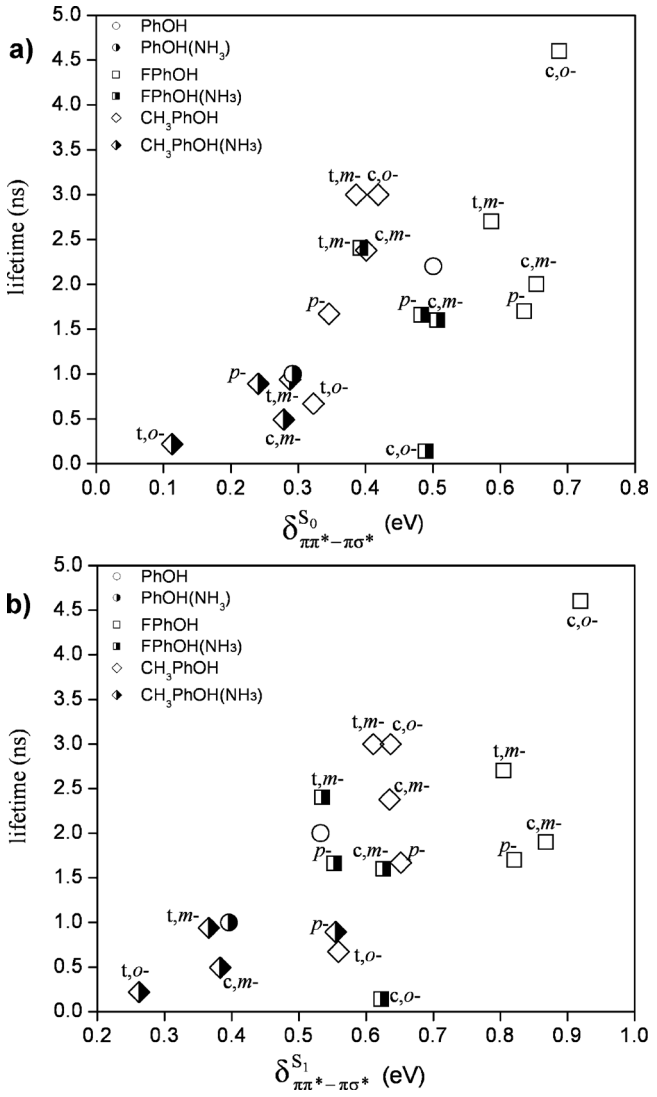

FIG. 4. Experimental S_1 state lifetimes determined for the vibrationless state of all the substituted X-PhOHs (X=H,F,CH_3) and their 1:1 complexes with NH_3 as a function of the energy gaps, between the $\pi\pi^*$ and the $\pi\sigma^*$ states, calculated (a) at the ground-state geometry and (b) at the S_1 state optimized geometry.

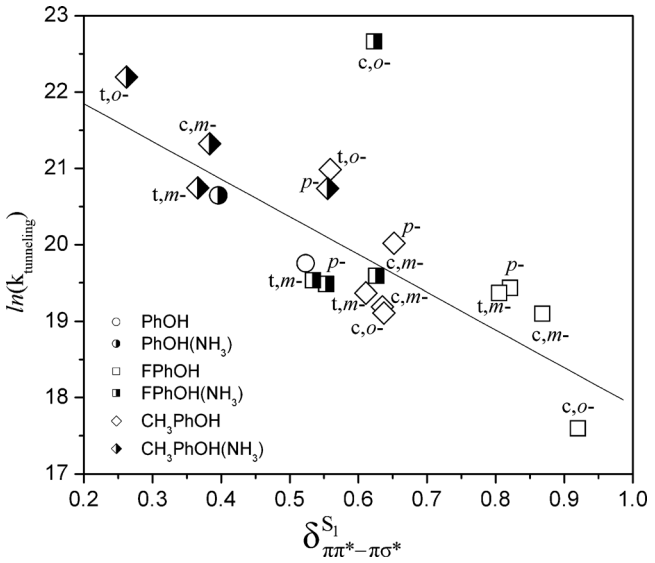

FIG. 5. Dependence of the $\ln(k_{tunneling})$ on the energy gap between the $\pi\pi^*$ and the $\pi\sigma^*$ states, calculated at the S_1 state optimized geometry, for all the substituted X-PhOHs (X=H,F,CH_3) and their 1:1 complexes with NH_3. The values of $k_{tunneling}$ were obtained from the experimental S_1 state lifetimes according to the description given in the text. The straight line is only a visual guide.

based on the $\pi\pi^*$-$\pi\sigma^*$ energy gap. This observation suggests that an additional effect must be considered to rationalize the increase of the ESHT rate in this complex. One possible reason is related to the fact that for c,*o*-F-PhOH(NH_3) the quantum chemical calculation reveals an important out-of-plane distortion of the C–F bond in the excited state S_1, as previously reported for the bare molecule.[33] This distortion reduces the symmetry from Cs to C1 and the discrimination between π^* and σ^* turns useless. Thus, $\pi\pi^*$ and $\pi\sigma^*$ states are expected to be completely mixed and consequently the ESHT reaction should be faster. This distortion occurs only in c,*o*-F-PhOH(NH_3), while the rest of the studied molecules and clusters hold the planar symmetry. The out-of-plane distortion of c,*o*-F-PhOH(NH_3) in the S_1 state is stabilized by a seven-member bridge structure where the ammonia molecule is hydrogen-bonded to the OH moiety of the chromophore molecule and simultaneously one of the NH bonds in ammonia forms a second hydrogen bond with the neighboring F atom. This additional hydrogen bond, only plausible due to the proximity between *ortho* OH and F groups, is thought to be the key to explain the characteristic dynamics of this cluster.

The out-of-plane distortion of c,*o*-F-PhOH(NH_3) in the S_1 state can be justified in terms of the vibronic coupling existing between the $\pi\pi^*$ and $\pi\sigma^*$ states that has previously been described for perfluorinated PhOHs (perfluoro effect).[42] Multiple substitution with fluorine atoms stabilizes the $\pi\sigma^*_F$ state toward the lower $\pi\pi^*$ state, where σ^*_F denotes the orbital localized on the C–F bond. When the low-lying $\pi\sigma^*_F$ state interacts with the $\pi\pi^*$ state through a certain out-of-plane vibrational mode (that compensate the symmetry difference between $\pi\pi^*$ and $\pi\sigma^*_F$), the potential curve of the $\pi\pi^*$ state becomes rather flat along that coordinate and consequently it exhibits a double minimum corresponding to the molecular geometries with the fluorine atom lying on each side of the plane of the aromatic ring. Such a distortion has been well analyzed in tetrafluorobenzene by the vibronic assignments and the comparison between one-photon and two-photon spectra[42] and the rotational analysis in the $S_1 \leftarrow S_0$ transitions.[43]

E. ESHD/T: Internal conversion or tunneling

The observed excited state lifetimes can be interpreted by two possible mechanisms for the H dissociation or transfer: either model A,[1] assuming a direct crossing from $\pi\pi^*$ to $\pi\sigma^*$ via tunneling through a barrier, or model B,[2] involving $S_1 \rightarrow S_0$ IC and subsequent transfer to the S_2 PES by nonadiabatic coupling near the S_0/S_2 conical intersection.

The possibility that the dissociation pathway involves direct hydrogen-atom tunneling across the potential energy barrier formed by the $\pi\pi^*$-$\pi\sigma^*$ states crossing was not considered in model B for the vibrationless level. We will show that this mechanism can also reproduce the order of magni-

tude of the measured S_1 lifetime of PhOH molecules and therefore it should be taken into account as a plausible dissociation channel. The probability of hydrogen tunneling can be estimated in terms of the Brillouin–Kramers–Wentzel semiclassical approximation, in which the transmission coefficient is given by

$$T_{BKW} = \exp\left(-2\int_{u1}^{u2}\sqrt{\frac{2m}{\hbar^2}(V(u)-E)}du\right) \quad (2)$$

where u represents the O−H coordinate and V(u)-E the one-dimensional potential barrier above the kinetic energy of the H atom, E. The function V(u) was taken from CASPT2 calculations done for the $\pi\pi^*$ and $\pi\sigma^*$ states[39,40] and E is half a quantum of the OH vibration (ZPE) in S_1. Numerical integration yields for T_{BKW} a value $\sim 10^{-5}$, which implies that the tunneling rate is about 10^9 s^{-1} and consequently the dissociation lifetime will be in the nanosecond range, in agreement with previous experimental and theoretical results.[12,13,37–40]

Previously, the excited state lifetime of naphthol$(NH_3)_n$ complexes had been estimated by assuming that the dissociation mechanism corresponds to an excited state proton transfer reaction controlled by tunneling.[41] Using a barrier width and height quite similar to the one calculated by King *et al.*,[40] ~50 ps tunneling time was predicted.

In the following paragraphs we will test the validity of the two models by comparing their results with the experimental observations.

1. Correlation between the $\pi\pi^*$-$\pi\sigma^*$ energy gap and the excited state lifetime.

As can be seen in Figs. 4 and 5, there is a correlation between the $\pi\pi^*$-$\pi\sigma^*$ energy gaps and the excited state lifetime for the free molecules and their complexes with NH_3. In model A,[1] the excited lifetimes for both complexes and free molecules are governed by the same parameters, the width and the height of the barrier along the O–H coordinate.

The dynamics of ESHT and ESHD are different in the final step, i.e., attachment of the H atom to NH_3 in complexes and H loss in the free molecules, and this will lead to different reaction rates. However, the first step which governs the excited state lifetime is similar in both reactions, or at least there is no special reason to change the model for each system studied, i.e., from the free molecule to the complex. In model B,[2] the excited state lifetime should only be linked to the IC mechanism which has no reason to be linked to the $\pi\pi^*$-$\pi\sigma^*$ energy gaps.

2. Different S_1 lifetimes of PhOH(NH_3) (1ns) (Ref. 25) and PhOH(H_2O)(15 ns) (Ref. 44) complexes and formation of a diradical with NH_3 and not with H_2O.

In model A,[1] the difference in lifetimes upon complexation with water or ammonia is explained in terms of the larger stability of NH_4 as compared to H_3O. With ammonia, the $PhOH^* + NH_3 \rightarrow PhO^\bullet + NH_4^\bullet$ reaction, which correlates with the $\pi\sigma^*$ state, is energetically allowed, while with water this reaction is energetically forbidden; thus, in the presence of water the lifetime of PhOH is governed by $S_1 \rightarrow S_0$ IC as in the case of deuterated PhOD. Consequently, deuterated PhOD and PhOH(H_2O) clusters have similar S_1 lifetimes. On the other hand, if the excited state lifetime is governed by internal conversion to S_0 as in model B (Ref. 2) the complexes with NH_3 and H_2O should have similar lifetimes.

3. Variation of the excited state lifetime of PhOH(NH_3) when the σ^1 band is excited.

As shown here, as well as in previous experiments,[7,25] excitation of the σ^1 band, i.e., the intermolecular $OH\cdots NH_3$ stretching mode, leads to a strong decrease of the S_1 lifetime. According to model A,[1] the excitation of this mode changes the width of the barrier and the tunneling probability as well as the reaction rate will also change. In model B (Ref. 2) the intermolecular excitation should not have any effect on the measured S_1 lifetime, which is linked to the IC via high ν_{OH} accepting modes.

4. Very short lifetime of c,o-F-PhOH(NH_3).

The very short lifetime of c,*o*-F-PhOH(NH_3) can be explained easily in terms of model A (Ref. 1) using a symmetry breaking argument. Since c,*o*-F-PhOH(NH_3) is nonplanar in the excited state, the $\pi\pi^*$ and $\pi\sigma^*$ states are strongly mixed (in fact they cannot be defined any more) resulting in a lower energy barrier for the H transfer, and consequently this reaction is accelerated. In model B,[2] S_0 and S_1 having the same symmetry, breakdown of the Cs symmetry should have no effect on the excited state lifetime.

In clusters, the experimental observations agree very well with a model of direct tunneling from the $\pi\pi^*$ state to the $\pi\sigma^*$ state, with a quite fast H tunneling in the PhOH(NH_3) cluster (1 ns lifetime). Since the $\pi\pi^*$-$\pi\sigma^*$ energy gaps are not too different in the complex and the free molecule, the H tunneling mechanism cannot be ruled out for the free molecule.

In summary, model A (Ref. 1) is simpler than model B,[2] it yields no contradiction with the observed data and it can explain observations that are difficult to explain using model B; therefore, we find no reason to invoke a more complicated mechanism. Moreover, we consider that the mechanism by which the system evolves from S_0 to S_2 in model B should be substantiated by further discussions, in particular the competition between the H loss and the IVR in S_0.

VI. CONCLUSIONS

The excited state lifetimes of fluorophenols, methylphenols, and their complexes with ammonia seem to be remarkably well correlated with the calculated $\pi\pi^*$-$\pi\sigma^*$ energy gaps. This propensity suggests that the excited state dynamics is governed by an excited state hydrogen detachment (ESHD) or transfer (ESHT) via H atom tunneling through a barrier.

ACKNOWLEDGMENTS

This work is supported by JSPS and MAE under the Japanese-France Integrated Action Program (SAKURA) and the CNRS/CONICET exchange program. E.M. thanks the CNRS for financial support. The authors thank Dr. A. L. Sobolewski and Dr. W. Domcke for helpful discussions.

[1] A. L. Sobolewski, W. Domcke, C. Dedonder-Lardeux, and C. Jouvet, Phys. Chem. Chem. Phys. **4**, 1093 (2002).
[2] M. N. R. Ashfold, B. Cronin, A. L. Devine, R. N. Dixon, and M. G. D. Nix, Science **312**, 1637 (2006).
[3] G. A. Pino, G. Grégoire, C. Dedonder-Lardeux, C. Jouvet, S. Martrenchard, and D. Solgadi, Phys. Chem. Chem. Phys. **2**, 893 (2000).
[4] G. A. Pino, C. Dedonder-Lardeux, G. Grégoire, C. Jouvet, S. Martrenchard, and D. Solgadi, J. Chem. Phys. **111**, 10747 (1999).
[5] S.-I. Ishiuchi, K. Daigoku, M. Saeki, M. Sakai, K. Hashimoto, and M. Fujii, J. Chem. Phys. **117**, 7077 (2002); **117**, 7083 (2002); K. Daigoku, S.-I. Ishiuchi, M. Sakai, M. Fujii, and K. Hashimoto, *ibid.* **119**, 5149 (2003); S.-I. Ishiuchi, M. Sakai, K. Daigoku, K. Hashimoto, and M. Fujii, *ibid.* **127**, 234304 (2007).
[6] O. David, C. Dedonder-Lardeux, C. Jouvet, H. Kang, S. Martrenchard, T. Ebata, and A. L. Sobolewski, J. Chem. Phys. **120**, 10101 (2004); O. David, C. Dedonder-Lardeux, C. Jouvet, and A. L. Sobolewski, J. Phys. Chem. A **110**, 9383 (2006); C. Dedonder-Lardeux, D. Grosswasser, C. Jouvet, and S. Martrenchard, PhysChemComm **4**, 21 (2001).
[7] O. David, C. Dedonder-Lardeux, and C. Jouvet, Int. Rev. Phys. Chem. **21**, 499 (2002).
[8] N. Tsuji, S.-I. Ishiuchi, M. Sakai, M. Fujii, T. Ebata, C. Jouvet, and C. Dedonder-Lardeux, Phys. Chem. Chem. Phys. **8**, 114 (2006).
[9] A. N. Oldani, J. C. Ferrero, and G. A. Pino, Phys. Chem. Chem. Phys. **11**, 10409 (2009).
[10] A. N. Oldani, M. Mobbili, E. Marceca, J. C. Ferrero, and G. A. Pino, Chem. Phys. Lett. **471**, 41 (2009).
[11] H. Lippert, V. Stert, C. P. Schulz, I. V. Hertel, and W. Radloff, Phys. Chem. Chem. Phys. **6**, 2718 (2004).
[12] M. G. D. Nix, A. L. Devine, B. Cronin, R. N. Dixon, and M. N. R. Ashfold, J. Chem. Phys. **125**, 133318 (2006).
[13] C.-M. Tseng, Y. T. Lee, and C. K. Ni, J. Chem. Phys. **121**, 2459 (2004); C.-M. Tseng, Y. T. Lee, M.-F. Lin, C.-K. Ni, S.-Y. Liu, P. Lee, Z. F. Xu, and M. C. Lin, J. Phys. Chem. A **111**, 9463 (2007); M. L. Hause, Y. H. Yoon, A. S. Case, and F. F. Crim, J. Chem. Phys. **128**, 104307 (2008); A. Iqbal, M. S. Y. Cheung, M. G. D. Nix, and V. G. Stavros, J. Phys. Chem. A **113**, 8157 (2009); A. Iqbal, L.-J. Pegg, and V. G. Stavros, *ibid.* **112**, 9531 (2008).
[14] A. L. Devine, M. G. D. Nix, B. Cronin, and M. N. R. Ashfold, Phys. Chem. Chem. Phys. **9**, 3749 (2007).
[15] G. A. King, A. L. Devine, M. G. D. Nix, D. E. Kelly, and M. N. R. Ashfold, Phys. Chem. Chem. Phys. **10**, 6417 (2008).
[16] C.-M. Tseng, Y. T. Lee, C.-K. Ni, and J.-L. Chang, J. Phys. Chem. A **111**, 6674 (2007).
[17] B. Cronin, M. G. D. Nix, R. H. Qadiri, and M. N. R. Ashfold, Phys. Chem. Chem. Phys. **6**, 5031 (2004).
[18] Z. Lan and W. Domcke, Chem. Phys. **350**, 125 (2008); Z. Lan, A. Dupays, V. Vallet, S. Mahapatra, and W. Domcke, J. Photochem. Photobiol., A **190**, 177 (2007).
[19] M.-F. Lin, C.-M. Tseng, Y. T. Lee, and C.-K. Ni, J. Chem. Phys. **123**, 024303 (2005).
[20] M.-F. Lin, C.-M. Tzeng, Y. A. Dyakov, and C.-K. Ni, J. Chem. Phys. **126**, 241104 (2007).
[21] M. G. D. Nix, A. L. Devine, B. Cronin, and M. N. R. Ashfold, Phys. Chem. Chem. Phys. **8**, 2610 (2006).
[22] A. Sur and P. M. Johnson, J. Chem. Phys. **84**, 1206 (1986).
[23] A. Carrera, I. B. Nielsen, P. Carcabal, C. Dedonder, M. Broquier, C. Jouvet, W. Domcke, and A. L. Sobolewski, J. Chem. Phys. **130**, 024302 (2009); G. Grégoire, C. Dedonder-Lardeux, C. Jouvet, S. Martrenchard, and D. Solgadi, J. Phys. Chem. A **105**, 5971 (2001).
[24] W. Domcke and A. L. Sobolewski, Science **302**, 1693 (2003); A. L. Sobolewski and W. Domcke, J. Phys. Chem. A **105**, 9275 (2001).
[25] G. Grégoire, C. Dedonder-Lardeux, C. Jouvet, S. Martrenchard, A. Peremans, and D. Solgadi, J. Phys. Chem. A **104**, 9087 (2000).
[26] M. Kawai and H. Nakai, Chem. Phys. **273**, 191 (2001).
[27] C. G. Hickman, J. R. Gascooke, and W. D. Lawrance, J. Chem. Phys. **104**, 4887 (1996).
[28] R. Ahlrichs, M. Bar, M. Haser, H. Horn, and C. Kolmel, Chem. Phys. Lett. **162**, 165 (1989).
[29] F. Weigend, M. Haser, H. Patzelt, and R. Ahlrichs, Chem. Phys. Lett. **294**, 143 (1998).
[30] O. Christiansen, H. Koch, and P. Jorgensen, Chem. Phys. Lett. **243**, 409 (1995).
[31] D. E. Woon and T. H. Dunning, Jr., J. Chem. Phys. **98**, 1358 (1993).
[32] E. Fujimaki, A. Fujii, T. Ebata, and N. Mikami, J. Chem. Phys. **110**, 4238 (1999); T. Aota, T. Ebata, and M. Ito, J. Phys. Chem. **93**, 3519 (1989); K. Suzuki, Y. Emura, S.-I. Ishiuchi, and M. Fujii, J. Electron Spectrosc. Relat. Phenom. **108**, 13 (2000).
[33] K. Remmers, W. L. Meerts, A. Zehnacker-Rentien, K. L. Barbu, and F. Lahmani, J. Chem. Phys. **112**, 6237 (2000).
[34] G. Myszkiewicz, W. L. Meerts, C. Ratzer, and M. Schmitt, J. Chem. Phys. **123**, 044304 (2005).
[35] G. Myszkiewicz, W. L. Meerts, C. Ratzer, and M. Schmitt, Phys. Chem. Chem. Phys. **7**, 2142 (2005).
[36] C. Ratzer, M. Nispel, and M. Schmitt, Phys. Chem. Chem. Phys. **5**, 812 (2003).
[37] C. Ratzer, J. Küpper, D. Spangenberg, and M. Schmitt, Chem. Phys. **283**, 153 (2002).
[38] Z. Lan, W. Domcke, V. Vallet, A. Sobolewski, and S. Mahapatra, J. Chem. Phys. **122**, 224315 (2005); O. P. J. Vieuxmaire, Z. Lan, A. L. Sobolewski, and W. Domcke, *ibid.* **129**, 224307 (2008).
[39] M. G. D. Nix, A. L. Devine, R. N. Dixon, and M. N. R. Ashfold, Chem. Phys. Lett. **463**, 305 (2008).
[40] G. A. King, T. A. A. Olivier, M. G. D. Nix, and M. N. R. Ashfold, J. Phys. Chem. A **113**, 7984 (2009).
[41] M. F. Hineman, G. A. Brucker, D. F. Kelley, and E. R. Bernstein, J. Chem. Phys. **97**, 3341 (1992).
[42] K. Okuyama, T. Kakinuma, M. Fujii, N. Mikami, and M. Ito, J. Phys. Chem. **90**, 3948 (1986).
[43] J. M. Hollas and M. Z. Binhussein, Chem. Phys. **124**, 297 (1988).
[44] R. J. Lipert, G. Bermudez, and S. D. Colson, J. Phys. Chem. **92**, 3801 (1988); G. A. Pino, in *Recent Advances in Nanoscience*, edited by M. M. Mariscal and S. A. Dassie (Research Signopost, Kerala, India, 2007), Chap. 5, p. 123.